



An AS1411 aptamer-conjugated liposomal system containing a bubble-generating agent for tumor-specific chemotherapy that overcomes multidrug resistance

Zi-Xian Liao ^{a,1}, Er-Yuan Chuang ^{b,1}, Chia-Chen Lin ^b, Yi-Cheng Ho ^c, Kun-Ju Lin ^{d,e}, Po-Yuan Cheng ^b, Ko-Jie Chen ^b, Hao-Ji Wei ^{f,g,*}, Hsing-Wen Sung ^{b,**}

^a Institute of Medical Science and Technology, National Sun Yat-sen University, Kaohsiung, Taiwan, ROC

^b Department of Chemical Engineering, Institute of Biomedical Engineering, National Tsing Hua University, Hsinchu, Taiwan, ROC

^c Department of Bioagriculture, National Chiayi University, Chiayi, Taiwan, ROC

^d Healthy Aging Research Center, Department of Medical Imaging and Radiological Sciences, College of Medicine, Chang Gung University, Taoyuan, Taiwan, ROC

^e Department of Nuclear Medicine, Molecular Imaging Center, Chang Gung Memorial Hospital, Taoyuan, Taiwan, ROC

^f Division of Cardiovascular Surgery, Veterans General Hospital—Taichung, College of Medicine, National Yang-Ming University, Taipei, Taiwan, ROC

^g Division of Cardiovascular Surgery, Chiayi Branch, Veterans General Hospital—Taichung, Chiayi, Taiwan, ROC

ARTICLE INFO

Article history:

Received 6 November 2014

Received in revised form 5 January 2015

Accepted 17 January 2015

Available online 28 January 2015

Chemical compounds studied in this article:

Dipalmitoylphosphatidylcholine
(PubChem CID: 6138)

Polyethylene glycol

2000-distearoylphosphatidylethanolamine
(PubChem CID: 406952)

Doxorubicin hydrochloride

(PubChem CID: 443939)

Ammonium bicarbonate

(PubChem CID: 14013)

¹⁸F-fluorodeoxyglucose

(PubChem CID: 450173)

Keywords:

Cancer therapy

Doxorubicin

Multidrug resistance

Thermoresponsive liposomes

Receptor-mediated endocytosis

ABSTRACT

Recent research in chemotherapy has prioritized overcoming the multidrug resistance (MDR) of cancer cells. In this work, liposomes that contain doxorubicin (DOX) and ammonium bicarbonate (ABC, a bubble-generating agent) are prepared and functionalized with an antinucleolin aptamer (AS1411 liposomes) to target DOX-resistant breast cancer cells (MCF-7/ADR), which overexpress nucleolin receptors. Free DOX and liposomes without functionalization with AS1411 (plain liposomes) were used as controls. The results of molecular dynamic simulations suggest that AS1411 functionalization may promote the affinity and specific binding of liposomes to the nucleolin receptors, enhancing their subsequent uptake by tumor cells, whereas plain liposomes enter cells with difficulty. Upon mild heating, the decomposition of ABC that is encapsulated in the liposomes enables the immediate activation of generation of CO₂ bubbles, creating permeable defects in their lipid bilayers, and ultimately facilitating the swift intracellular release of DOX. *In vivo* studies in nude mice that bear tumors demonstrate that the active targeting of AS1411 liposomes can substantially increase the accumulation of DOX in the tumor tissues relative to free DOX or passively targeted plain liposomes, inhibiting tumor growth and reducing systemic side effects, including cardiotoxicity. The above findings indicate that liposomes that are functionalized with AS1411 represent an attractive therapeutic alternative for overcoming the MDR effect, and support a potentially effective strategy for cancer therapy.

© 2015 Elsevier B.V. All rights reserved.

* Correspondence to: H.J. Wei, Division of Cardiovascular Surgery, Veterans General Hospital—Taichung, College of Medicine, National Yang-Ming University, Taipei, Taiwan, ROC.

** Correspondence to: H.W. Sung, Department of Chemical Engineering, National Tsing Hua University, Hsinchu 30013, Taiwan, ROC.

E-mail addresses: weihaoji@vghc.gov.tw (H.-J. Wei), hwsung@mx.nthu.edu.tw (H.-W. Sung).

¹ The first two authors (Z.X. Liao and E.Y. Chuang) contributed equally to this work.

1. Introduction

Despite its high antitumor activity, the effectiveness of doxorubicin (DOX) is severely limited by the development of the multidrug resistance (MDR) of cancer cells that arises from the overexpression of their plasma membrane P-glycoprotein (P-gp) transporters, which actively increases the drug efflux [1]. One strategy for solving this problem is to bypass the efflux-mediated MDR effect by conjugating a targeting ligand onto the surface of the delivery vehicles so that they can be taken up by the tumor cells *via* receptor-mediated endocytosis.

Liposomes that incorporate with polyethylene glycol (PEG)-conjugated lipids have been used as a stable vehicle for carrying DOX (i.e. the Doxil® formulation) for the treatment of various cancers [2–5]. PEGylation has been shown to help prevent the rapid clearance of liposomes by the reticuloendothelial system and prolong their blood circulation time [6]. Systemically administered vehicles must firstly flow through the vasculature towards the tumor and then extravasate *via* the enhanced permeability and retention (EPR) effect [7], eventually accumulating within the tumor. However, the release of the drug from the Doxil® formulation is typically slow (<10% in 24 h), owing to the lack of a triggering mechanism, considerably limiting its cytotoxic effects on tumor cells [8–10].

To address the above concern, our group has recently developed a thermoresponsive liposomal system that can locally control and rapidly trigger drug release [11]. The key component of this liposomal system is its encapsulated ammonium bicarbonate (ABC; NH_4HCO_3), which can be used to establish the transmembrane gradient that is required for the highly efficient encapsulation of DOX by remote-loading [12]. Furthermore, upon mild hyperthermia at approximately 42 °C, the ABC that is encapsulated in the aqueous compartment of liposomes decomposes rapidly to generate CO_2 bubbles, converting the liposome membranes into permeable defects, which yield a high drug concentration at the tumor interstitium. Clinically, local hyperthermia may be produced by ultrasound energy, microwave, radiofrequency, or using magnetic hyperthermia [13]. After diffusing into tumor cells and eventually entering the cell nuclei, DOX molecules bind strongly to nuclear DNA, killing the cells. Notably, most normal tissues remain unharmed following treatment for 1 h at temperatures up to 44 °C [14]. The results of our previous animal study demonstrated that these thermoresponsive ABC liposomes exhibited greater antitumor activity than the temperature-insensitive liposomes that resemble the Doxil® formulation, revealing the importance of the intratumoral release of DOX from the delivery vehicles.

In this work, liposomes that contain DOX hydrochloride and ABC are prepared and functionalized with an antinucleolin aptamer (AS1411) for targeting DOX-resistant MCF-7 breast cancer cells (MCF-7/ADR) that overexpress nucleolin receptors [15]. AS1411 is a 26-nucleotide guanosine-rich DNA aptamer that can bind to the nucleolin proteins

on tumor cells and enter those cells when the nucleolin receptors are shuttled from the plasma membrane into the cytoplasm [16]. Once the liposomes have been internalized by the cancer cells, local heating generates CO_2 bubbles by the decomposition of ABC, rapidly triggering the release of DOX from the liposomal carriers. The rapid intracellular drug release significantly increases the amount of subsequently accumulated DOX in the nuclei beyond the threshold to kill the cancer cells (Scheme 1).

AS1411-functionalized liposomes (AS1411 liposomes) were characterized using dynamic light scattering (DLS) and ultrasonography; their drug release behavior, receptor-mediated cellular uptake, intracellular trafficking, and subsequent accumulation of DOX were examined *in vitro* by fluorescence microscopy, molecular dynamic (MD) simulations, flow cytometry, and confocal laser scanning microscopy (CLSM), respectively. The liposomes without functionalization with AS1411 (plain liposomes) served as a control. Following the establishment of an MCF-7/ADR xenograft model in athymic nude mice, the *in vivo* drug accumulation of each test liposomal formulation at the tumor site and its therapeutic efficacy against locally heated tumors were investigated.

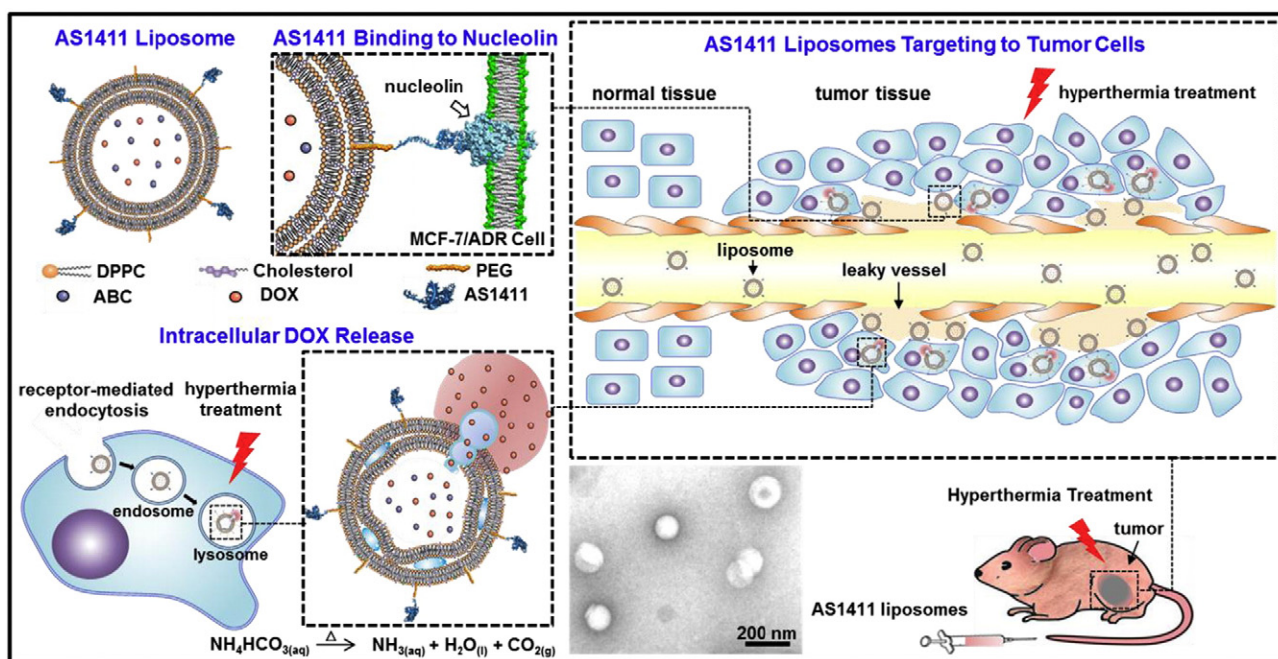
2. Materials and methods

2.1. Materials

Dipalmitoylphosphatidylcholine (DPPC) and polyethylene glycol 2000-distearoylphosphatidylethanolamine (PEG 2000-DSPE) were purchased from Avanti Polar Lipids (Alabaster, AL, USA); DOX was obtained from Fisher Scientific (Waltham, MA, USA), and ABC and cholesterol were acquired from Sigma-Aldrich (St. Louis, MO, USA). The DOX-resistant MCF-7/ADR cell line was obtained from the Biomedical Technology and Device Research Laboratories, Hsinchu, Taiwan. All other chemicals and reagents used were of analytical grade.

2.2. Preparation of test liposomes

In this work, test liposomes were prepared by film hydration followed by sequential extrusion. To prepare the liposomes without



Scheme 1. Schematic illustrations displaying the structure of an AS1411 liposome and its specific binding to nucleolin on cell surface, subsequent receptor-mediated endocytosis, and intracellular DOX accumulation activated by formation of CO_2 bubbles *via* thermal decomposition of encapsulated ABC. Consequent cytotoxicity inhibits growth of tumor cells. A TEM micrograph of the AS1411 liposomes is also included.

functionalization with AS1411 (plain liposomes), DPPC, cholesterol and PEG 2000-DSPE in a molar ratio of 60:40:5 were dissolved in chloroform and placed in a high vacuum to remove the residual organic solvent. The lipid film thus obtained was then hydrated using an aqueous ABC solution (2.7 M) *via* sonication at room temperature, which was followed by sequential extrusions at room temperature to control the size of the obtained liposomes [17]. Our previously conducted small-angle X-ray scattering analysis indicated that the as-prepared liposomes were multilamellar vesicles with two or three lamellae [11].

To prepare the test liposomes that were functionalized with AS1411 (AS1411 liposomes), thiol-containing AS1411 was firstly conjugated to maleimide-PEG 2000-DSPE, in a 1:5 molar ratio, *via* the formation of a thioether linkage [18]. The unreacted AS1411 was removed by five rounds of centrifugation using a membrane ultrafiltration filter tube (Vivaspin 2, MWCO: 3 kDa; GE Healthcare, Buckinghamshire, UK). The purified conjugates self-assembled into spherical micelles. These micelles were then incubated with the above-mentioned plain liposomes (in a 1:5 molar ratio of maleimide-PEG 2000-DSPE:PEG 2000-DSPE) under sonication at room temperature for 30 min, allowing the micelle components to be exchanged into the liposome bilayers [19].

To load the drug, DOX was mixed with the as-prepared liposomal suspensions at a drug-to-lipid ratio of 0.05 (by w/w), which was maintained at room temperature for 24 h. The drug-loaded liposomes were then passed through a G-25 column (GE Healthcare) to remove the unencapsulated DOX.

2.3. Characterization of test liposomes

The mean particle size and zeta potential of the plain and AS1411 liposomes were measured by DLS (Zetasizer 3000HS; Malvern Instruments, Worcestershire, UK), while the DOX encapsulation efficiency and content in each test formulation were determined by making fluorescence measurements (Spex FluoroMax-3; Horiba Jobin Yvon, Edison, NJ, USA) after the test liposomes had been destroyed with Triton X-100. The thermoresponsive characteristics of test liposomes were elucidated by examining the formation of CO₂ bubbles in a test tube that contained the liposomes in phosphate-buffered saline (PBS, pH 7.4) at body (37 °C) and hyperthermic temperatures (42 °C). The test tubes that contained the samples were immersed in a water-filled tank, and the generation of CO₂ bubbles was studied using an ultrasound imaging system (Z-one, Zonare; Mountain View, CA, USA).

The DOX release profiles were obtained by immersing the test liposomes (10 mg/mL, 50 µL) in quartz cells that contained 1 mL PBS, which were gently shaken in a thermostatic rotary shaker at 100 rpm and 37 °C or 42 °C. Samples were removed at predetermined intervals, and an equal amount of the same medium was added to maintain a constant volume. The amount of DOX released from the test liposomes was analyzed using fluorescence spectrometry.

2.4. MD simulations of molecular interactions of AS1411 and nucleolin

MD simulations of the interactions between AS1411 and the nucleolin receptor on the plasma membrane were conducted using the program NAMD with parameters adapted from those of the CHARMM 27 force field [20,21], and the binding energy of AS1411 and the receptor was determined by performing geometrical route simulations [22]. The details of the procedure can be found in our earlier publication [23].

2.5. Receptor-mediated cellular uptake

MCF-7/ADR cells were maintained in Eagle's medium that was supplemented with 10% fetal bovine serum, 1% L-glutamine, and 1% penicillin streptomycin at pH 7.4 and 37 °C in a humidified incubation chamber with 5% CO₂. The receptor-mediated cellular uptake of test liposomes was analyzed by flow cytometry. The cells were treated with the DiO-

labeled plain or AS1411-functionalized liposomes. Following incubation for predetermined periods at 37 °C, test samples were aspirated. To verify that the receptor-mediated endocytosis was mainly responsible for the cellular uptake of AS1411 liposomes, a competitive assay in which free AS1411 was pre-incubated with MCF-7/ADR cells prior to treatment with the test liposomes, was conducted. The cells were then carefully washed three times by pre-warmed PBS, fixed in 4% paraformaldehyde, and detached by 0.025% trypsin/EDTA. Finally, the detached cells were introduced into a flow cytometer that was equipped with a 488 nm argon laser (Beckman Coulter, Fullerton, CA, USA) to determine their uptake of the fluorescence-labeled liposomes.

2.6. Intracellular trafficking of test liposomes, accumulation of DOX, and cytotoxicity

To monitor the intracellular trafficking of drug carriers, MCF-7/ADR cells were seeded in 35 mm dishes with a cover-slip glass bottom (1.5×10^5 cells/dish) and incubated overnight. Next, the cells were rinsed twice with culture medium and treated with the DiO-labeled AS1411 liposomes (1 mg/mL). After they had been incubated again for predetermined durations, the cells were washed twice with PBS before being fixed in 4% paraformaldehyde. The fixed cells were then examined using immunohistochemical staining to identify nucleolin, endosomes (EEA1), and lysosomes (LAMP2) and they were counterstained by DAPI to visualize the nuclei, before being observed with a CLSM (Zeiss LSM780, Carl Zeiss, Jena GmbH, Germany).

To evaluate the intracellular DOX accumulation, MCF-7/ADR cells were treated with the test liposomes at both temperatures (37 °C and 42 °C). Following incubation, the cells were washed twice with pre-warmed PBS and then fixed in 4% paraformaldehyde. The intracellular accumulation of DOX was studied using CLSM. Additionally, the amount of DOX accumulated in cells was quantified by flow cytometry, and their cell viability was determined by the MTT assay [24].

2.7. Animal model

Nude mice (BALB/cAnN.Cg-Foxn1nu/CrlNarl, 6–8 weeks old) were acquired from the National Laboratory Animal Center, Taiwan. Use and the care of experimental animals were in compliance with the "Guide for the Care and Use of Laboratory Animals", prepared by the Institute of Laboratory Animal Resources, National Research Council, and published by the National Academy Press. The Institutional Animal Care and Use Committee of National Tsing Hua University approved the study protocol (no. 10177). The MCF-7/ADR cells (5×10^6 cells in 100 µL Matrigel; BD Biosciences, Franklin Lakes, NJ) were implanted subcutaneously in the left flank region of athymic nude mice [25].

2.8. In vivo DOX accumulation and its antitumor efficacy

When the tumors had grown to a mean volume of around 200 mm³, the mice were divided into six groups and each was injected intravenously in the tail under one of the following experimental conditions (n = 6 per group): no treatment (untreated control); free DOX; plain liposomes alone; plain liposomes + hyperthermia treatment (42 °C); AS1411 liposomes alone; or AS1411 liposomes + hyperthermia treatment. In the hyperthermically treated groups, at 4 h following intravenous injection, the tumor site was locally heated to 42 °C. A circulation time of approximately 4 h has been reported to be ideal for liposomes to allow them accumulating in a tumor through the EPR effect [26]. The dose of DOX under each test condition was 0.2 mg per kg body weight once every 4 days for four times. Local hyperthermia treatment was performed using a temperature-controller water mat. Periods of hyperthermia (10 min) were alternated with 5 min cooling periods three times. At 4 h after the treatment, the mice were sacrificed, and their organs and tumors were harvested and visualized using an

in vivo imaging system (IVIS; Xenogen, Alameda, CA, USA) to monitor qualitatively the *in vivo* DOX accumulation. An aqueous solution (10 mL) containing deionized water and ethanol (50:50 v/v) was added to each test tissue. The mixture was then homogenized and centrifuged at 14,000 rpm for 30 min; the supernatant was lyophilized and resuspended in 1 mL deionized water. Finally, the fluorescence intensity of the solution was quantified using a spectrofluorometer (F-2500; Hitachi, Tokyo, Japan).

To evaluate the antitumor efficacy for each treatment modality, the above process was repeated every four days and a total of four treatments were conducted. The tumor sizes and body weights of each test group were measured every other day and normalized to their initial values. Tumor size was determined using a caliper, and tumor volume was calculated using the following equation: $V = (\pi / 6) \times LW^2$, where L denotes the long diameter and W represents the short diameter [27].

At the end of the repeated treatments, the mice were fasted overnight and then anesthetized with isoflurane (2% in 100% O₂), before being injected with 0.32 mCi ¹⁸F-fluorodeoxyglucose (¹⁸F-FDG) in 100 μL of saline *via* the tail vein. A 10 min image acquisition was carried out 1 h after ¹⁸F-FDG injection using a positron emission tomographic (PET) scanner (Inveon™, Siemens Medical Solutions, Knoxville, TN, USA). Finally, the mice were sacrificed, and the tumor tissues were retrieved and fixed in 4% neutral buffered formalin, embedded in paraffin, sectioned, and stained with hematoxylin–eosin (H&E). TUNEL assays were performed using an *in situ* cell death detection kit (Roche Diagnostics GmbH, Mannheim, Germany).

2.9. Statistical analysis

All results are presented as mean ± SD. The Student *t* test was conducted to compare the means of pairs of groups. Comparisons of more than two groups were made by one-way ANOVA followed by the Bonferroni post hoc test. Differences were considered to be statistically significant when $P < 0.05$.

3. Results and discussion

Recent research in chemotherapy has strongly prioritized mitigating the MDR effect in cancer cells, which is responsible for the high recurrence rate in chemotherapy and its ultimate failure. Accordingly, a liposomal formulation whose surface is functionalized with a DNA aptamer (AS1411) is developed herein. The surface-functionalized AS1411 can bind to nucleolin, a receptor protein that is overexpressed on the plasma membrane of some drug-resistant tumor cells (such as MCF-7/ADR cells), enhancing their uptake of liposomes; it therefore has the advantages of bypassing the P-gp-mediated drug efflux and reducing the MDR effect of cancer cells. To trigger a rapid drug release in cells, a thermoresponsive bubble-generating agent, ABC, is also encapsulated in the aqueous core of AS1411 liposomes. This study evaluates the effectiveness of AS1411-functionalized liposomes in binding to the nucleolin receptors of MCF-7/ADR cells and their ability to deliver DOX intracellularly to build up a concentration that exceeds the cell-killing threshold. Plain liposome counterparts, without functionalization with AS1411, are used as a control.

3.1. Characteristics of test liposomes

DLS was used to evaluate the sizes and surface potentials of the as-prepared liposomes. AS1411 conjugation increased liposome size ($P < 0.05$; Table 1), suggesting that the presence of an additional hydrophilic molecule on the liposomal surface increased the hydrodynamic radius. Meanwhile, the negatively charged DNA aptamer reduced the surface potential of the liposomes ($P < 0.05$). The remote-loading technique, which exploits the transmembrane gradient of ABC [25], revealed an efficient and stable loading of DOX (>90% encapsulation efficiency) into the aqueous compartment of each test liposomal formulation. Furthermore, both test liposomes contained the same concentration of DOX ($P > 0.05$), which was approximately 100 times the saturated concentration of DOX in water.

ABC is utilized as a raising agent in the food industry to produce gas bubbles in baked goods [28]. Heating (>40 °C) causes ABC to decompose rapidly into water, ammonia, and CO₂ bubbles [29,30]. Since gas bubbles are hyperechogenic [31], the generation of CO₂ bubbles from the test liposomes that contain ABC can be observed using an ultrasound imaging system. When stored at 4 °C, no CO₂ bubbles were observed from the plain and AS1411 liposomes for at least 4 weeks. According to Fig. 1a, a few CO₂ bubbles were detected in the samples of both test liposomes at 37 °C (body temperature), while a large number of CO₂ bubbles were observed immediately following heating of the environmental temperature of the liposomes to 42 °C (hyperthermic temperature). These experimental results reveal that both plain and AS1411 liposomes underwent a unique temperature-induced change by the thermal decomposition of their encapsulated ABC, enabling the immediate formation of CO₂ bubbles, which created permeable defects in the lipid bilayers of the liposomes, ultimately facilitating the swift local release of DOX.

Fig. 1b presents the *in vitro* DOX release profiles of the plain and AS1411 liposomes at both test temperatures, which were obtained by measuring the increases in the fluorescence intensities of DOX in PBS over time. At 37 °C, the amounts of DOX that were released from both test liposomes were relatively low; however, when the local temperature was increased to 42 °C, significant amounts of encapsulated DOX were quickly released. These results indicate that both plain and AS1411 liposomes were relatively stable at body temperature. However, when the environmental temperature was raised, the liposomes released the drug extremely fast, yielding a high local drug concentration. Notably, the amount of DOX that was released from the AS1411 liposomes was relatively higher than the plain liposomes, suggesting that the surface-bound hydrophilic aptamer made the liposomes slightly unstable. Similar findings have been reported elsewhere [32].

3.2. MD simulations of binding of test liposomes to nucleolin

AS1411 is known to bind to nucleolin with high affinity; however, the corresponding molecular interactions are still not well understood. MD simulations were conducted to elucidate the mechanism by which the liposome with or without AS1411 interacts with the nucleolin on the plasma membrane. Fig. 2 shows pictures of complexes of the two interacting molecules at the atomic resolution, and Table 2 presents their corresponding binding energies. The formation of a stable DNA (AS1411)–protein (nucleolin) complex depends on a negative binding

Table 1

Characteristics of plain and AS1411 liposomes. Data are presented as mean ± SD ($n = 6$ in each group). Encapsulation efficiency: (mass of DOX in liposomes / mass of DOX in initial solution) × 100%; encapsulation content: (mass of DOX in liposomes / mass of lipids) × 100%.

Test samples	Diameter (nm)	Zeta potential (mV)	Encapsulation efficiency (%)	Encapsulation content (%)
Plain liposomes	127.1 ± 31.8	0.5 ± 0.1	96.2 ± 6.1	4.8 ± 0.3
AS1411 liposomes	172.2 ± 43.9	−7.8 ± 3.3	92.1 ± 4.7	4.6 ± 0.2

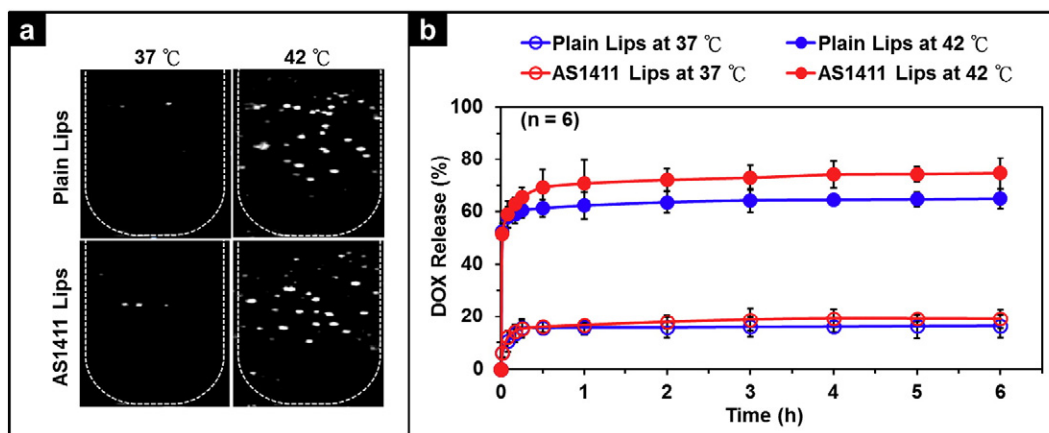


Fig. 1. (a) Ultrasound images of plain and AS1411 liposomes (lips) suspended in aqueous media, maintained at body temperature (37 °C) or hyperthermic temperature (42 °C), (b) corresponding *in vitro* release profiles of DOX.

energy, and a more negative binding energy corresponds to an increase in binding affinity [33].

According to Table 2, the binding energy for the PEG–nucleolin complex was slightly negative, suggesting that the interaction between the plain liposome and the nucleolin receptor was not that favorable. In contrast, the AS1411–nucleolin complex had the largest negative binding energy of any of the investigated complexes, suggesting that the

interaction between the AS1411 liposome and the nucleolin protein would be the most spontaneous and stable, as confirmed by the MD simulation results. (See Supplementary Video.) AS1411 has a stable G-quadruplex structure, allowing it to bind to its target protein with high affinity and specificity [34]. Following pretreatment with AS1411, the negatively charged DNA aptamer blocked the nucleolin receptor on the plasma membrane, which thus became inaccessible to the

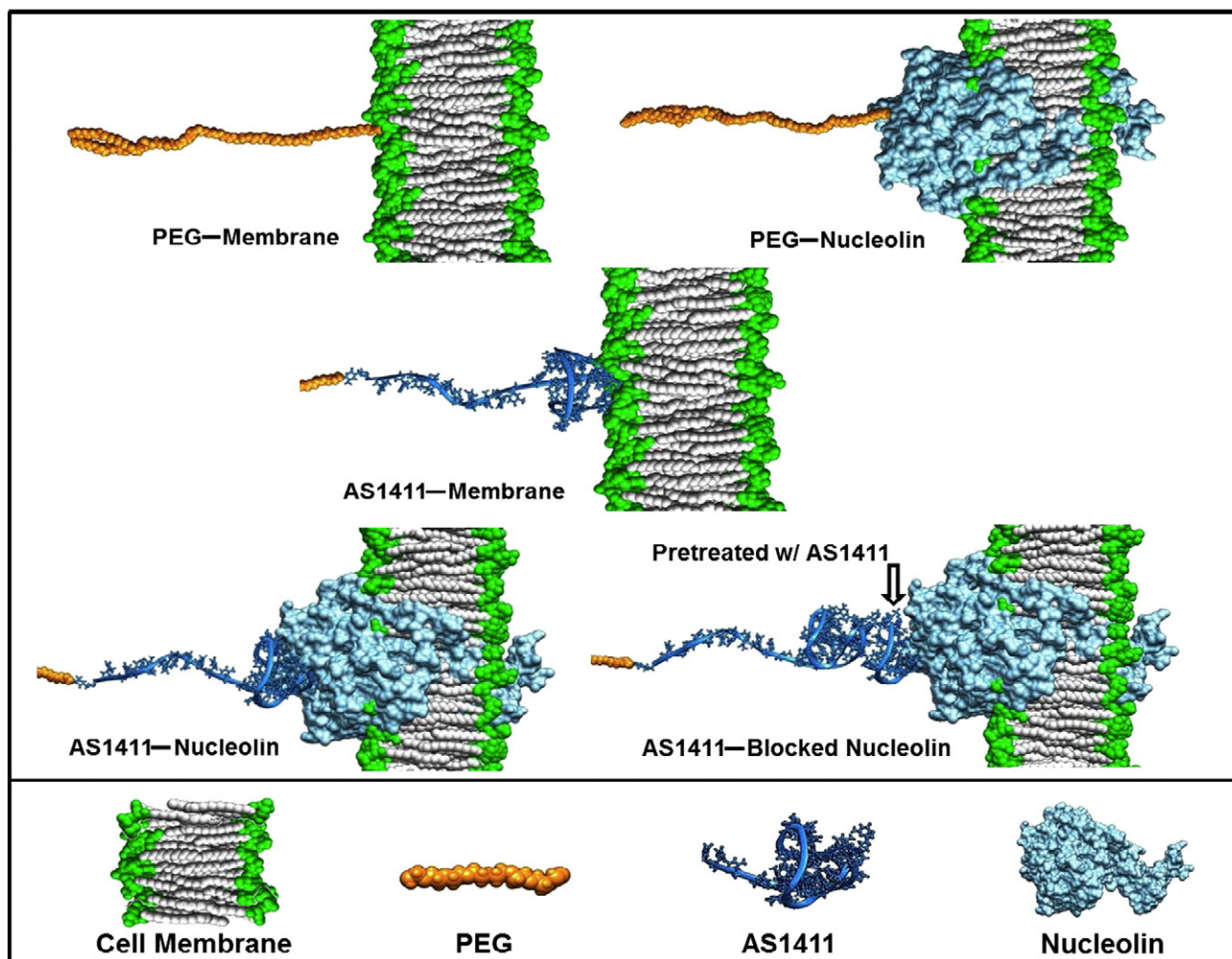


Fig. 2. (a) Results of molecular dynamic simulations, showing conformation of two interacting test molecules.

Table 2

Binding energies (kcal/mol) of molecular interactions between two test molecules, determined by geometrical route simulations.

Test samples	Binding energy
PEG–membrane	-5.4 ± 0.8
PEG–nucleolin	-27.8 ± 27.2
AS1411–membrane	-51.6 ± 22.8
AS1411–nucleolin	-1711.0 ± 36.9
AS1411–blocked nucleolin	60.5 ± 5.6

AS1411 liposome (negatively charged, as shown in Table 1), as revealed by the positive binding energy. The above results indicate that AS1411 may promote the high affinity and specific binding of test liposomes to nucleolin receptors, enhancing their subsequent cellular uptake via a receptor-mediated endocytosis pathway.

3.3. Receptor-mediated cellular uptake of AS1411-functionalized liposomes

After binding to the cell surface receptors, aptamers and their conjugated drug vehicles undergo endocytosis [35]. The possible role of AS1411 in the receptor-mediated cellular uptake of test liposomes was also explored in the study. The fluorescent intensities of the cells that internalized the DiO-labeled plain or AS1411 liposomes were quantified by flow cytometry. Based on Fig. 3a, the observed intensity of fluorescence in the group that had been treated with the plain liposomes was minimal throughout the study, suggesting that the plain liposomes that contained PEG 2000-DSPE had difficulty in entering the tumor cells. As is well known, the incorporation of PEG-lipids prolongs the circulation half-life of liposomes but inhibits their cellular uptake [36,37]. Hence, upon hyperthermia treatment, the release of DOX from the plain liposomes is mostly extracellular. Like free DOX, the extracellular release of DOX at the drug-resistant tumor site may be prone to the MDR effect, and an effective dose may not be deliverable intracellularly.

Conversely, the group receiving the AS1411-functionalized liposomes produced an increased fluorescent intensity as incubation progressed, revealing a considerably greater cellular uptake which is essential to enhance the intracellular drug concentration. Following the pretreatment of the cells with AS1411 (blocking their plasma membrane nucleolin), the extent of the cellular uptake of AS1411 liposomes became similar to that of plain liposomes ($P > 0.05$). These experimental results demonstrate that conjugating AS1411 can significantly augment the internalization of test liposomes, most likely via the nucleolin receptor-mediated endocytosis pathway.

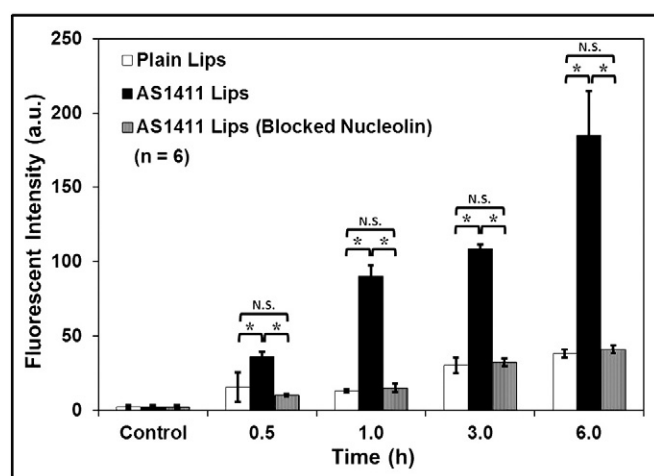


Fig. 3. Fluorescent intensities of MCF-7/ADR cells after they had been incubated with DiO-labeled plain or AS1411 liposomes (lips) for predetermined durations, revealing extent of cellular uptake; results for cells that had been pretreated with AS1411 to block nucleolin membrane protein are also presented. N.S.: statistically insignificant; *statistical significance at a level of $P < 0.05$.

3.4. Intracellular trafficking of internalized AS1411 liposomes, accumulation of DOX, and cytotoxicity

The intracellular trafficking of the internalized particles was tracked by the co-localization of intracellular organelles and the AS1411 liposomes that had been labeled with DiO, which served as a fluorescence probe to locate the test liposomes. The results thus obtained suggest that AS1411-functionalized liposomes entered the cells after binding to the nucleolin receptors at 10 min post-culture and transported to early endosomes (EEA1) at 20 min and, finally, to lysosomes (LAMP2) at 30 min (Fig. 4a).

The kinetics of the DOX accumulation in cells treated with the AS1411 liposomes was also visualized by CLSM. As time passed, faint red fluorescence signals (DOX) were detected in the nuclear region of the MCF-7/ADR cells at 37 °C (Fig. 4b). In the absence of an external triggering mechanism, the drug may be released from a liposomal carrier by degrading the carrier in the late endosome or lysosome, and this process is typically quite slow [38]. In contrast, subsequent to local hyperthermia treatment at 42 °C, a significant amount of DOX rapidly accumulated in the cell nuclei, and this process was activated by the formation of CO₂ bubbles via the thermal decomposition of the encapsulated ABC.

Analyzed by flow cytometry, the quantitative results of DOX accumulated in MCF-7/ADR cells that had been treated with free DOX, plain liposomes or AS1411 liposomes are summarized in Fig. 4c. As compared to the untreated control, the DOX fluorescence intensities accumulated in the cells receiving free DOX or plain liposomes were relatively low at both test temperatures, reflecting the drug efflux by the P-gp transporters. Conversely, the accumulation of DOX in the cells treated with the AS1411 liposomes at hyperthermic temperature increased remarkably ($P < 0.05$). Above results indicate that AS1411 liposomes were less susceptible to the P-gp-mediated drug efflux and thus can assist DOX accumulation in the cell nuclei, where it has its cytotoxic effect [39]. After treatments, the mitochondrial activity of living cells was measured by the MTT assay. According to Fig. 4d, the cell viability declined significantly when treating of the AS1411 liposomes with local heating ($P < 0.05$).

3.5. In vivo DOX accumulation

The accumulation of DOX in tissues following an intravenous injection of free DOX, plain liposomes, or AS1411 liposomes via the tail veins of tumor-bearing mice was examined. Following treatment, the mice were sacrificed, and their organs, including the tumors, were harvested and then visualized using an IVIS system (Fig. 5a). The intensities of their fluorescence were quantified using a spectrofluorometer (Fig. 5b).

The tumors that received free DOX yielded much weaker DOX fluorescence signals than did those treated with the plain or AS1411 liposomes. Only the hearts of the free DOX-treated animals yielded a detectable DOX signal, perhaps reflecting unacceptable cardiotoxicity [40]. The DOX signals from the tumors in mice that received plain liposomes at body temperature (37 °C) were relatively weak but increasing the temperature of the tumor enhanced the intensity of its DOX fluorescence. The tumors in the groups that were treated with AS1411 liposomes yielded significantly stronger DOX signals at both test temperatures, and especially when heated locally ($P < 0.05$). These findings suggest that AS1411 liposomes were successfully delivered to the tumor tissues and, upon mild heating, decomposition of their encapsulated ABC facilitated the immediate thermal formation of CO₂ bubbles, leading to a possible intracellular accumulation of DOX.

3.6. Antitumor activity

Finally, the effectiveness of the various liposomal formulations in suppressing the growth of MCF-7/ADR tumors in nude mice was explored. The group with no treatment and that received free DOX served

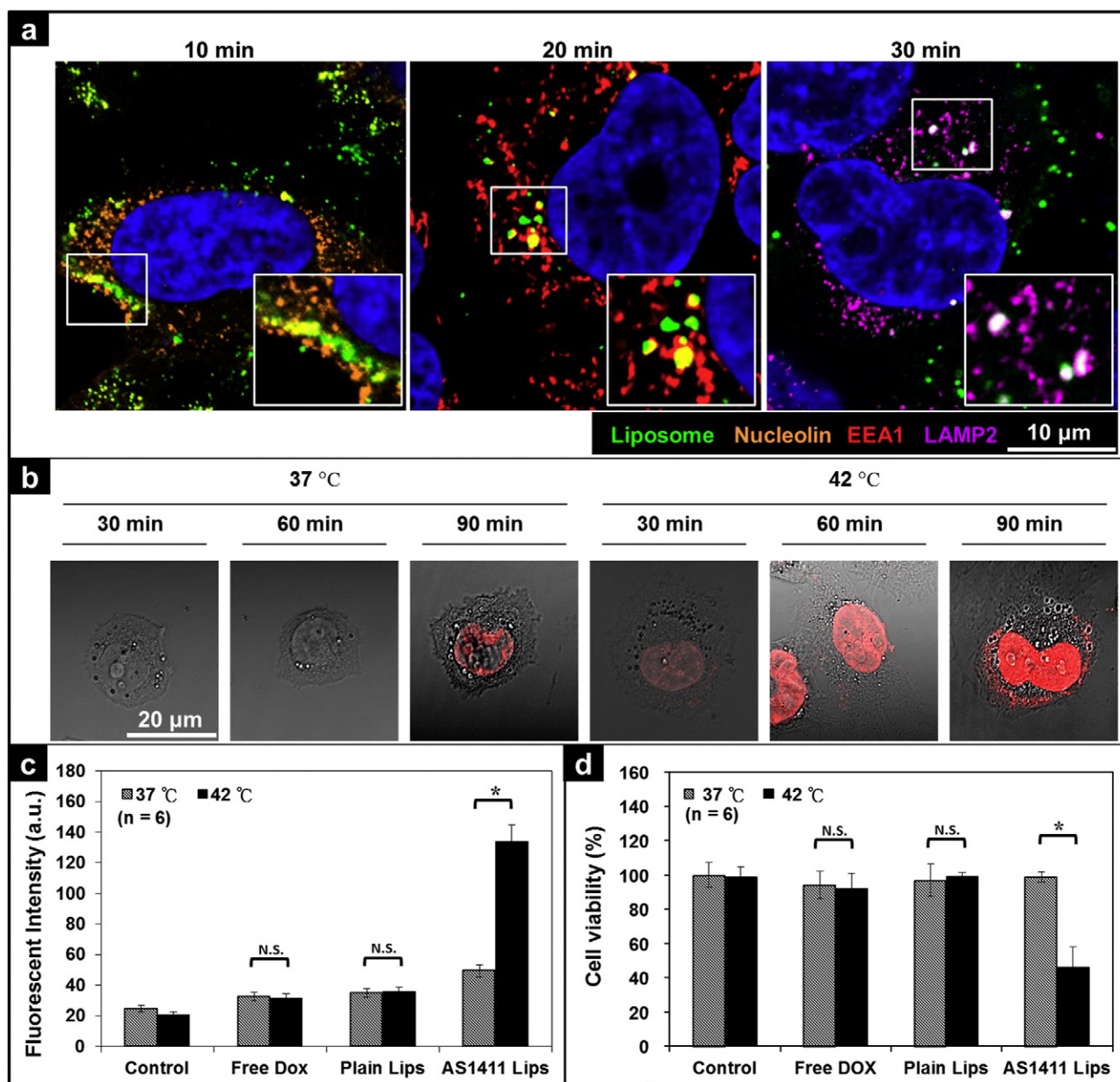


Fig. 4. (a) CLSM images of intracellular trafficking of AS1411 liposomes in MCF-7/ADR cells. Inset magnifies area within square. (b) CLSM images of accumulations of DOX in MCF-7/ADR cells after they had been incubated with AS1411 liposomes for predetermined durations at 37 °C or 42 °C. (c) Results of DOX accumulated in cells treated with free DOX, plain liposomes, or AS1411 liposomes at 37 °C or 42 °C, analyzed by flow cytometry, and (d) their cell viability determined by the MTT assay. N.S.: statistically insignificant; *statistical significance at a level of $P < 0.05$.

as controls. Like the untreated control, free DOX exhibited minimal antitumor activity against the drug-resistant tumors (Fig. 6a). Treatment with plain or AS1411 liposomes alone provided significantly less antitumor efficacy than the respective treatment with local heating ($P < 0.05$). Unable to release their encapsulated DOX promptly and adequately, owing to the lack of a triggering mechanism, these stable liposomal formulations had suboptimal cytotoxic effects on the tumor cells. With mild local heating, the AS1411 liposomes suppressed tumor growth more did the plain liposomes because the former caused more of the drug to accumulate at the target tumor (Figs. 6a and b). Therapeutic effects are maximized only when the tumor cells are subjected to the maximum concentration of a drug [41].

At the end of treatments, the antitumor ability of AS1411 liposomes combined with local heating was further examined using a PET scanner and by histological analyses of tumor sections. ^{18}F -FDG has been extensively employed as a contrast agent for the PET imaging of tumors [42].

The uptake of ^{18}F -FDG by tumor tissue depends on its metabolic activity. When tumor cells die, a decline in their ^{18}F -FDG uptake is expected. ^{18}F -FDG images in Fig. 6b revealed a significant reduction in uptake by the tumor that was treated with AS1411 liposomes with local heating ($2.81 \pm 0.97\%$ ID/g), compared to that of the untreated control (5.45 ± 0.68 ID/g) or the group that was treated with free DOX (4.50 ± 0.44 ID/g), revealing a reduction in metabolic activity of the cells.

By comparison with the untreated control, tumor tissues that had been treated with AS1411 liposomes + local heating – but not those that received free DOX – exhibited signs of significant cell destruction, including a low nuclear-to-cytoplasmic ratio (H&E stain) and a large number of TUNEL-positive cells (Fig. 7). Furthermore, myofibrillar loss and cytoplasmic vacuolization (H&E stain) with TUNEL-positive cardiomyocytes were clearly observed in mice that had been treated with free DOX. In contrast, little evidence of cardiomyocyte pathological

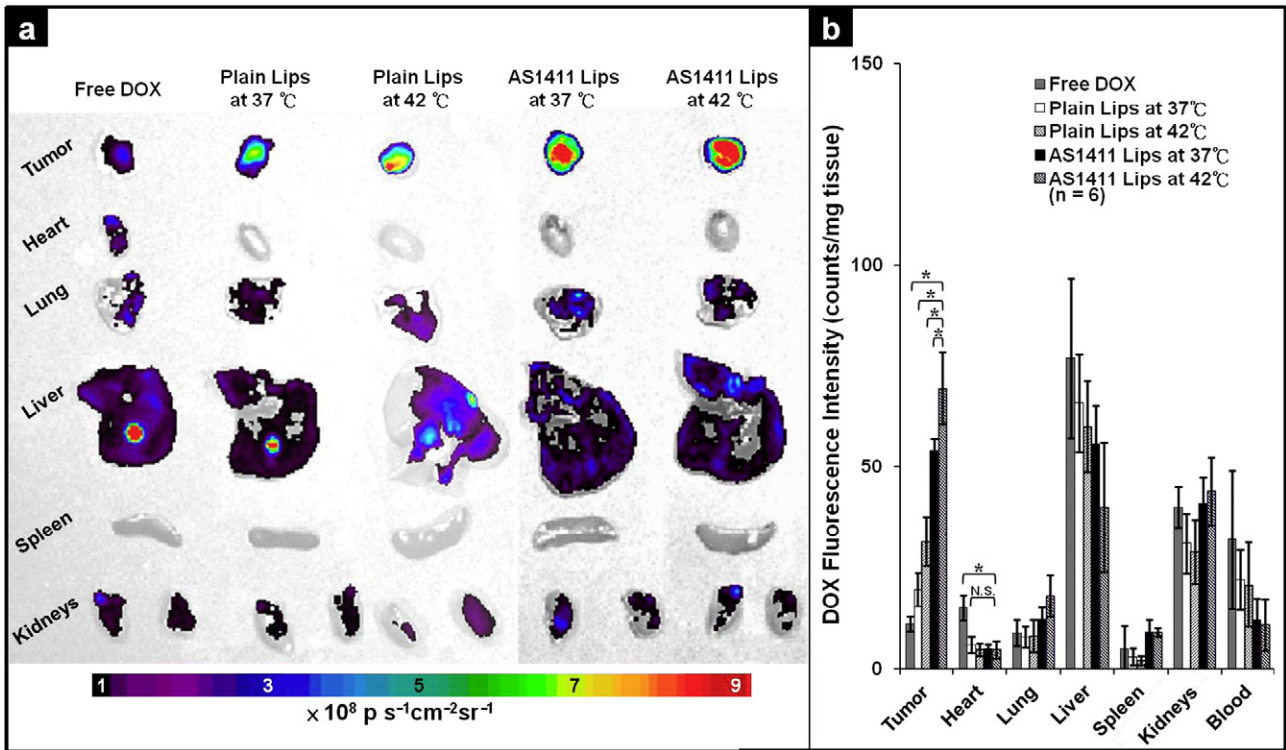


Fig. 5. (a) Fluorescent images of DOX accumulated in organs and tumors following intravenous injection of mice with free DOX, plain liposomes, or AS1411 liposomes, with or without hyperthermia treatments, and (b) corresponding fluorescent intensities quantified using a spectrofluorometer. N.S.: statistically insignificant; *statistical significance at a level of $P < 0.05$.

changes in mice that received AS1411 liposomes + local hyperthermia treatment was obtained. These empirical data demonstrate that the encapsulation of DOX by AS1411 liposomes with mild local heating

inhibited tumor growth and reduced systemic side effects, including cardiotoxicity, providing a potentially effective strategy for cancer therapy.

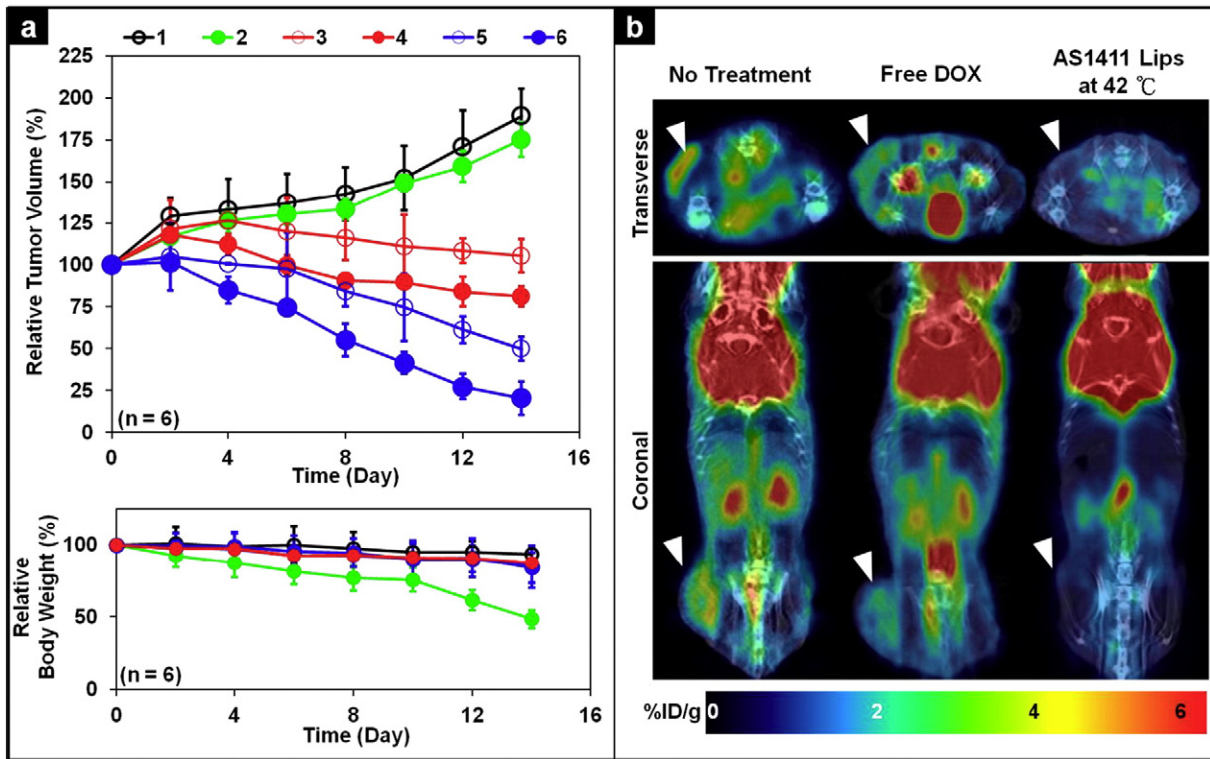


Fig. 6. (a) Changes in relative tumor volume and body weight of mice bearing MCF-7/ADR tumors upon various treatments (1: no treatment; 2: free DOX; 3: plain liposomes alone; 4: plain liposomes + hyperthermia treatment; 5: AS1411 liposomes alone; 6: AS1411 liposomes + hyperthermia treatment). (b) ¹⁸F-FDG PET/CT co-registered images of mice following various treatments. Tumor site is indicated by white arrowhead.

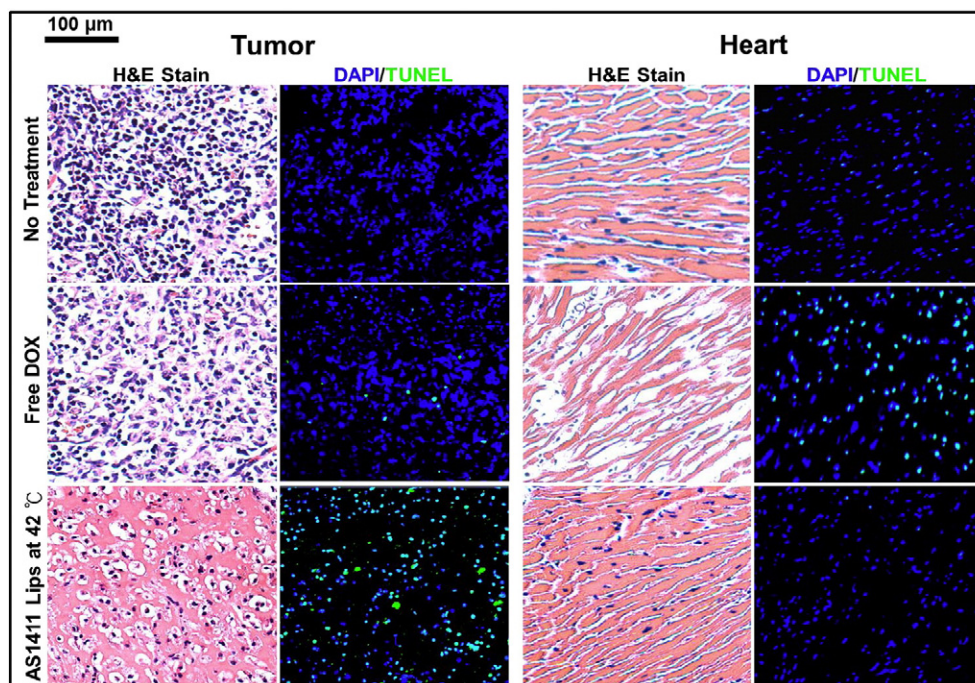


Fig. 7. Histological photomicrographs of tumor and heart sections stained with H&E, and corresponding TUNEL staining of apoptotic cells for groups that underwent various treatments.

4. Conclusions

Functionalizing the surface of liposomes with an antinucleolin aptamer (AS1411) significantly enhances their cellular uptake by cancer cells. Encapsulating ABC, a bubble-generating agent, in their aqueous core enables rapid drug release when triggered via local heating, markedly increasing the subsequent accumulation of DOX in the cell nuclei beyond the threshold for killing the cancer cells. The specific receptor-mediated endocytosis together with a thermoresponsive drug release mechanism in cells, which overcomes the MDR effect of cancer cells that is afforded by the unique design of this liposomal formulation, result in improved therapeutic outcomes and reduced systemic toxicity.

Supplementary data to this article can be found online at <http://dx.doi.org/10.1016/j.jconrel.2015.01.032>.

Acknowledgments

This work was supported by a grant from the National Science Council (NSC 103-2221-E-007-022-MY3), Taiwan (ROC). The PET-imaging study was supported by grants from the Chang Gung Memorial Hospital at Linkou (CMRPG300161 and CMRPG391513), Taiwan.

References

- [1] L.W. Fu, Y.M. Zhang, Y.J. Liang, X.P. Yang, Q.C. Pan, The multidrug resistance of tumor cells was reversed by tetrandrine *in vitro* and in xenografts derived from human breast adenocarcinoma MCF-7/ADR cells, *Eur. J. Cancer* 38 (2002) 418–426.
- [2] Y. Barenholz, Doxil®—the first FDA-approved nano-drug: lessons learned, *J. Control. Release* 160 (2012) 117–134.
- [3] X. Li, Q. Zhao, L. Qiu, Smart ligand: aptamer-mediated targeted delivery of chemotherapeutic drugs and siRNA for cancer therapy, *J. Control. Release* 171 (2013) 152–162.
- [4] T.A. Elbayoumi, V.P. Torchilin, Tumor-targeted nanomedicines: enhanced antitumor efficacy *in vivo* of doxorubicin-loaded, long-circulating liposomes modified with cancer-specific monoclonal antibody, *Clin. Cancer Res.* 15 (2009) 1973–1980.
- [5] D. Pornpattananangkul, S. Olson, S. Aryal, M. Sartor, C.M. Huang, K. Vecchio, L. Zhang, Stimuli-responsive liposome fusion mediated by gold nanoparticles, *ACS Nano* 4 (2010) 1935–1942.
- [6] K. Maruyama, Intracellular targeting delivery of liposomal drugs to solid tumors based on EPR effects, *Adv. Drug Deliv. Rev.* 63 (2011) 161–169.
- [7] M.K. Danquah, X.A. Zhang, R.I. Mahato, Extravasation of polymeric nanomedicines across tumor vasculature, *Adv. Drug Deliv. Rev.* 63 (2011) 623–639.
- [8] T.M. Allen, P.R. Cullis, Drug delivery systems: entering the mainstream, *Science* 303 (2004) 1818–1822.
- [9] G.L. Plosker, Pegylated liposomal doxorubicin: a review of its use in the treatment of relapsed or refractory multiple myeloma, *Drugs* 68 (2008) 2535–2551.
- [10] K.M. Laginha, S. Verwoert, G.J. Charrois, T.M. Allen, Determination of doxorubicin levels in whole tumor and tumor nuclei in murine breast cancer tumors, *Clin. Cancer Res.* 11 (2005) 6944–6949.
- [11] K.J. Chen, H.F. Liang, H.L. Chen, Y. Wang, P.Y. Cheng, H.L. Liu, Y. Xia, H.W. Sung, A thermoresponsive bubble-generating liposomal system for triggering localized extracellular drug delivery, *ACS Nano* 7 (2013) 438–446.
- [12] G. Haran, R. Cohen, L.K. Bar, Y. Barenholz, Transmembrane ammonium sulfate gradients in liposomes produce efficient and stable entrapment of amphipathic weak bases, *Biochim. Biophys. Acta* 1151 (1993) 201–215.
- [13] C.D. Landon, J.Y. Park, D. Needham, M.W. Dewhirst, Nanoscale drug delivery and hyperthermia: the materials design and preclinical and clinical testing of low temperature-sensitive liposomes used in combination with mild hyperthermia in the treatment of local cancer, *Open Nanomed. J.* 3 (2011) 38–64.
- [14] M.F. Chung, K.J. Chen, H.F. Liang, Z.X. Liao, W.T. Chia, Y. Xia, H.W. Sung, A liposomal system capable of generating CO₂ bubbles to induce transient cavitation, lysosomal rupturing, and cell necrosis, *Angew. Chem. Int. Ed.* 51 (2012) 10089–10093.
- [15] S. Soundararajan, W. Chen, E.K. Spicer, N. Courtenay-Luck, D.J. Fernandes, The nucleolin targeting aptamer AS1411 destabilizes Bcl-2 messenger RNA in human breast cancer cells, *Cancer Res.* 68 (2008) 2358–2365.
- [16] A. Aravind, P. Jeyamohan, R. Nair, S. Veerananarayanan, Y. Nagaoka, Y. Yoshida, T. Maekawa, D.S. Kumar, AS1411 aptamer tagged PLGA-lecithin-PEG nanoparticles for tumor cell targeting and drug delivery, *Biotechnol. Bioeng.* 109 (2012) 2920–2931.
- [17] P.J. Patty, B.J. Frisken, The pressure-dependence of the size of extruded vesicles, *Biophys. J.* 85 (2003) 996–1004.
- [18] D. Peters, M. Kastantin, V.R. Kotamraju, P.P. Karmali, K. Gujrati, M. Tirrell, E. Ruoslahti, Targeting atherosclerosis by using modular, multifunctional micelles, *Proc. Natl. Acad. Sci. U. S. A.* 106 (2009) 9815–9819.
- [19] J. Takasaki, S.M. Ansell, Micelles as intermediates in the preparation of protein-liposome conjugates, *Bioconjug. Chem.* 17 (2006) 438–450.
- [20] M.T. Nelson, W. Humphrey, A. Gursoy, A. Dalke, L.V. Kale, R.D. Skeel, K. Schulten, NAMD: a parallel, object oriented molecular dynamics program, *Int. J. High Perform. Comput. Appl.* 10 (1996) 251–268.
- [21] B.R. Brooks, R.E. Bruccoleri, B.D. Olafson, D.J. States, S. Swaminathan, M. Karplus, CHARMM: a program for macromolecular energy, minimization, and dynamics calculations, *J. Comput. Chem.* 4 (1983) 187–217.
- [22] W. Jiang, B. Roux, Free energy perturbation Hamiltonian replica-exchange molecular dynamics (FEP/H-REMD) for absolute ligand binding free energy calculations, *J. Chem. Theory Comput.* 6 (2010) 2559–2565.
- [23] L.W. Hsu, Y.C. Ho, E.Y. Chuang, C.T. Chen, J.H. Juang, F.Y. Su, S.M. Hwang, H.W. Sung, Effects of pH on molecular mechanisms of chitosan-integrin interactions and resulting tight-junction disruptions, *Biomaterials* 34 (2013) 784–793.
- [24] C.J. Ke, W.L. Chiang, Z.X. Liao, H.L. Chen, P.S. Lai, J.S. Sun, H.W. Sung, Real-time visualization of pH-responsive PLGA hollow particles containing a gas-generating agent targeted for acidic organelles for overcoming multi-drug resistance, *Biomaterials* 34 (2013) 1–10.

- [25] K.J. Chen, E.Y. Chuang, S.P. Wey, K.J. Lin, F. Cheng, C.C. Lin, H.L. Liu, H.W. Tseng, C.P. Liu, M.C. Wei, C.M. Liu, H.W. Sung, Hyperthermia-mediated local drug delivery by a bubble-generating liposomal system for tumor-specific chemotherapy, *ACS Nano* 8 (2014) 5105–5115.
- [26] G.A. Koning, A.M. Eggermont, L.H. Lindner, T.L. Ten Hagen, Hyperthermia and thermosensitive liposomes for improved delivery of chemotherapeutic drugs to solid tumors, *Pharm. Res.* 27 (2010) 1750–1754.
- [27] R.W. Ahn, F. Chen, H. Chen, S.T. Stern, J.D. Clogston, A.K. Patri, M.R. Raja, E.P. Swindell, V. Parimi, V.L. Cryns, T.V. O'Halloran, A novel nanoparticulate formulation of arsenic trioxide with enhanced therapeutic efficacy in a murine model of breast cancer, *Clin. Cancer Res.* 16 (2010) 3607–3617.
- [28] B. Min, I.Y. Bae, H.G. Lee, S.H. Yoo, S. Lee, Utilization of pectin-enriched materials from apple pomace as a fat replacer in a model food system, *Bioresour. Technol.* 101 (2010) 5414–5418.
- [29] Y. Yang, N. Bajaj, P. Xu, K. Ohn, M.D. Tsifansky, Y. Yeo, Development of highly porous large PLGA microparticles for pulmonary drug delivery, *Biomaterials* 30 (2009) 1947–1953.
- [30] A. Boddien, F. Gartner, C. Federsel, P. Sponholz, D. Mellmann, R. Jackstell, H. Junge, M. Beller, CO₂-“neutral” hydrogen storage based on bicarbonates and formates, *Angew. Chem. Int. Ed.* 50 (2011) 6411–6414.
- [31] S.L. Huang, Liposomes in ultrasonic drug and gene delivery, *Adv. Drug Deliv. Rev.* 60 (2008) 1167–1176.
- [32] D. Liu, L.M. Bimbo, E. Makila, F. Villanova, M. Kaasalainen, B. Herranz-Blanco, C.M. Caramella, V.P. Lehto, J. Salonen, K.H. Herzig, J. Hirvonen, H.A. Santos, Co-delivery of a hydrophobic small molecule and a hydrophilic peptide by porous silicon nanoparticles, *J. Control. Release* 170 (2013) 268–278.
- [33] M.N. Davies, C.E. Sansom, C. Beazley, D.S. Moss, A novel predictive technique for the MHC class II peptide-binding interaction, *Mol. Med.* 9 (2003) 220–225.
- [34] S. Soundararajan, L. Wang, V. Sridharan, W. Chen, N. Courtenay-Luck, D. Jones, E.K. Spicer, D.J. Fernandes, Plasma membrane nucleolin is a receptor for the anticancer aptamer AS1411 in MV4-11 leukemia cells, *Mol. Pharmacol.* 76 (2009) 984–991.
- [35] B.L. Zhang, Z. Luo, J.J. Liu, X.W. Ding, J.H. Li, K.Y. Cai, Cytochrome c end-capped mesoporous silica nanoparticles as redox-responsive drug delivery vehicles for liver tumor-targeted triplex therapy *in vitro* and *in vivo*, *J. Control. Release* 192 (2014) 192–201.
- [36] D. Pozzi, V. Colapicchioni, G. Caracciolo, S. Piovesana, A.L. Capriotti, S. Palchetti, S. De Grossi, A. Riccioli, H. Amenitsch, A. Lagana, Effect of polyethyleneglycol (PEG) chain length on the bio-nano-interactions between PEGylated lipid nanoparticles and biological fluids: from nanostructure to uptake in cancer cells, *Nanoscale* 6 (2014) 2782–2792.
- [37] J. Xie, C. Xu, N. Kohler, Y. Hou, S. Sun, Controlled PEGylation of monodisperse Fe₃O₄ nanoparticles for reduced non-specific uptake by macrophage cells, *Adv. Mater.* 19 (2007) 3163–3166.
- [38] D.C. Drummond, O. Meyer, K.L. Hong, D.B. Kirpotin, D. Papahadjopoulos, Optimizing liposomes for delivery of chemotherapeutic agents to solid tumors, *Pharmacol. Rev.* 51 (1999) 691–743.
- [39] K. Shao, Q.S. Hou, W. Duan, M.L. Go, K.P. Wong, Q.T. Li, Intracellular drug delivery by sulfatide-mediated liposomes to gliomas, *J. Control. Release* 115 (2006) 150–157.
- [40] T.M. Suter, M.S. Ewer, Cancer drugs and the heart: importance and management, *Eur. Heart J.* 34 (2013) 1102–1111.
- [41] T.M. Allen, Ligand-targeted therapeutics in anticancer therapy, *Nat. Rev. Cancer* 2 (2002) 750–763.
- [42] A.K. Buck, G. Halter, H. Schirrmeister, J. Kotzerke, I. Wurzigler, G. Glatting, T. Mattfeldt, B. Neumaier, S.N. Reske, M. Hetzel, Imaging proliferation in lung tumors with PET: ¹⁸F-FLT versus ¹⁸F-FDG, *J. Nucl. Med.* 44 (2003) 1426–1431.